

AD-A191 897

SIMULATION OF MATCHED FIELD PROCESSING CONVERGENCE
ZONES IN A STRONG BOTTOM FIELD (U) NAVAL OCEAN SYSTEMS
CENTER SAN DIEGO CA D F GORDON NOV 87

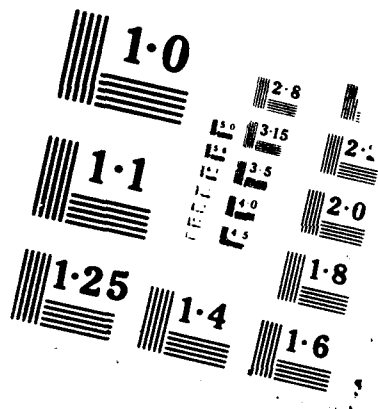
1/1

UNCLASSIFIED

F/G 28/1

NL





AD-A191 897

DTIC FILE COPY

①

UN
SEC

REPORT DOCUMENTATION PAGE

1a. REPORT SECURITY CLASSIFICATION UNCLASSIFIED			1b. RESTRICTIVE MARKINGS			
2a. SECURITY CLASSIFICATION AUTHORITY			3. DISTRIBUTION/AVAILABILITY OF REPORT Approved for public release; distribution is unlimited.			
2b. DECLASSIFICATION/DOWNGRADING SCHEDULE			4. PERFORMING ORGANIZATION REPORT NUMBER(S)			
4. PERFORMING ORGANIZATION REPORT NUMBER(S)			5. MONITORING ORGANIZATION REPORT NUMBER(S)			
6a. NAME OF PERFORMING ORGANIZATION Naval Ocean Systems Center		6b. OFFICE SYMBOL (if applicable) NOSC		7a. NAME OF MONITORING ORGANIZATION Naval Ocean Systems Center		
6c. ADDRESS (City, State and ZIP Code) San Diego, CA 92152-5000			7b. ADDRESS (City, State and ZIP Code) San Diego, CA 92152-5000			
8a. NAME OF FUNDING SPONSORING ORGANIZATION		8b. OFFICE SYMBOL (if applicable)		9. PROCUREMENT INSTRUMENT IDENTIFICATION NUMBER		
8c. ADDRESS (City, State and ZIP Code)			10. SOURCE OF FUNDING NUMBERS			
			PROGRAM ELEMENT NO	PROJECT NO	TASK NO	AGENCY ACCESSION NO
			In-house			
11. TITLE (include Security Classification) Simulation of Matched Field Processing for Convergence Zones in a Strong Bottom Field						
12. PERSONAL AUTHOR(S) D. F. Gordon						
13a. TYPE OF REPORT Presentation/speech		13b. TIME COVERED FROM May 87 TO May 87		14. DATE OF REPORT (Year, Month, Day) November, 1987		15. PAGE COUNT
16. SUPPLEMENTARY NOTATION						
17. COSATI CODES			18. SUBJECT TERMS (Continue on reverse if necessary and identify by block number)			
FIELD	GROUP	SUB-GROUP	sum beamforming target vectors convergence zone energy.			
19. ABSTRACT (Continue on reverse if necessary and identify by block number) Below 30 Hz the convergence zone energy can be smaller than the bottom reflected energy. Matched field simulations using a normal mode program give narrow, irregular correlation peaks for target vectors taken from the complete field. Target vectors computed using only modes representing convergence zone energy are then processed against the complete acoustic field. A much broader, smoother correlation function is obtained. Target vectors are then constructed that are equivalent to delay and sum beamforming at specified angles. These vectors give correlation functions that resembled those for convergence zone energy, and illustrate the relationship between matched field processing and beamforming.						
20. DISTRIBUTION AVAILABILITY OF ABSTRACT <input type="checkbox"/> UNCLASSIFIED UNLIMITED <input checked="" type="checkbox"/> SAME AS RPT <input type="checkbox"/> DTIC USERS				21. ABSTRACT SECURITY CLASSIFICATION UNCLASSIFIED		
22a. NAME OF RESPONSIBLE INDIVIDUAL D. F. Gordon			22b. TELEPHONE (include Area Code) (619)225-6301		22c. OFFICE SYMBOL Code 711	

DTIC ELECTED
S MAR 28 1988
D
E

Simulation of matched field processing for convergence zones in a strong bottom field. David F. Gordon, (Naval Ocean Systems Center, Code 711, San Diego, CA 92152-5000)

Below 30 Hz the convergence zone energy can be smaller than the bottom reflected energy. Matched field simulations using a normal mode program give narrow, irregular correlation peaks for target vectors taken from the complete field. Target vectors computed using only modes representing convergence zone energy are then processed against the complete acoustic field. A much broader, smoother correlation function is obtained. Target vectors are then constructed that are equivalent to delay and sum beamforming at specified angles. These vectors give correlation functions that resembled those for convergence zone energy, and illustrate the relationship between matched field processing and beamforming.

Suggestion for special session on Matched Field Signal Processing

Technical Committee: Underwater Sound

Method of Presentation: Prefer lecture but willing to give as poster

(PACS) Subject Classification numbers: 43.60.Gk, 43.30.Es

Telephone number 619/225-6301

Send acceptance or rejection notice to D. F. Gordon

Accession For	
NTIS GRA&I	<input checked="" type="checkbox"/>
DTIC TAB	<input type="checkbox"/>
Unannounced	<input type="checkbox"/>
Justification	
By _____	
Distribution/	
Availability Codes	
Dist	Avail and/or Special
A-1	

88 3 25 08 9

Simulation of Matched Field Processing for Convergence Zones
in a Strong Bottom Field

by D. F. Gordon

To be delivered at the 113th Meeting of the Acoustical Society of America, Indianapolis, Indiana, Session DD, 14 May 1987

In most wave theory computations of underwater sound propagation the convergence zone (cz) only field can be computed much more easily and accurately than can a complete field that includes bottom reflected energy. For this reason the effect of using the cz only field on matched field processing was investigated. The investigation was extended to other simplified descriptions of the matching field including simple fields equivalent to alternating polarity arrays. Some results of this investigation will be reported here.

At frequencies below 30 Hz the bottom reflected field may be stronger than the cz field at the range of the second cz. This is illustrated in the first two viewgraphs. Viewgraph 1 shows a contoured propagation loss field showing the first and second cz. Also shown are the depth of the 16 elements of a vertical array. The spacing between elements is $1/2$ wavelength at 30 Hz. We will be interested later on in the pressure amplitude along the array. Note the indication here that there will be alternating intervals of high and low amplitude down the array.

The contoured field we see here is for a 100m deep source and the array is at 100 km range. Sound pressures shown here are computed by a normal mode program for a Pacific profile at 30 Hz frequency. A very lossy bottom, modeled as a negative gradient half space, was used to suppress bottom reflected energy.

Viewgraph 2 shows a similar computation, but here a realistic bottom was used. The bottom was modeled as two fluid layers representing 70m of fine grained sediment over rock. Note that the convergence zones can still be distinguished, but are distorted by the bottom reflected energy.

The array at 100 km range is again shown. The 16 pressures, expressed as complex numbers, for this source depth of 100 m and this range will be used as the target vector. The 16 pressures for each point on the total grid of source depths and ranges constitutes the field vectors.

Let us first look at the results of simulating matched field processing for this total field case. The total grid comprises the range points and 10 different source depths from 20 to 200m. Viewgraph 3 shows the result of this simulation. The contours are the squared absolute value of the correlation coefficient between the 16 pressures at the target vector and any field vector. The expected high correlation can be seen at 100m source depth and 100m range. However, there are many secondary peaks nearby, which in the presence of noise might be mistaken for the primary peak.

We will now inquire into the effect of using a cz only field. This will be done by substituting the sound pressures computed in this way for the

target vector. The best simulation of reality would require that the numerous field vectors rather than the target vector be re-computed by the method being considered. However, to minimize computing, the field vectors are always the same, computed from the total field. It is assumed that results for the two methods will differ in detail but be similar in general behavior.

Viewgraph 4 repeats viewgraph 3 but for an enlarged view. Here we see the true target point at 100 km range and also a second area of enhanced correlation at 10 km greater range. This turns out to be a location where the upgoing rays at the target have refracted and are returning downward in a similar pattern. The cz only target vector correlation will now be shown on this same scale.

Viewgraph 5 shows this matched field. Note first that we no longer have a 100 percent correlation point. In fact, the target location no longer is the strongest correlation. This occurs for about 80m greater source depth. This correlation function is much smoother and more massive than the previous full field one. However, it no longer has the source localization properties of the previous one. Again we see the downgoing part of the cz about 10 km farther in range.

Let us now briefly look at the correlation process. Viewgraph 6 shows the correlation equation. Here t is the target vector and p is the field vector. The summations are over the 16 array elements. Note that t can also be thought of as the weights and delays for an ordinary plane wave beam former. The value of the correlation is then the response of the beamformer to a source at the source depth and range of the field vector. In the remainder of this paper the target vector will be viewed interchangeable in these two ways.

Viewgraph 7 shows the sound pressure from element to element down the array. The complex pressure is shown as an amplitude and phase. The left hand plot is the pressures of the cz only target vector used previously. Note the alternating high and low amplitude down the array. There is a tendency for the phase to advance 180° from one amplitude peak to the next. The right hand plot is the pressure that would be set up by two equal plane waves intersecting the array from 10° above and below the horizontal. The interference pattern set up down the array is a sine wave. A comparison of these two plots indicates that the cz pressures have a strong component of two plane waves near $+10^\circ$. The overall amplitude of the target vector is normalized out of the correlation function so it is only the relative amplitude and phase that matter in the target vector. However, the location of the sine wave pattern in depth along the array is a significant parameter and depends upon the relative phase of the two interfering plane waves. Here, their relative phase has been chosen to match the computed target vector.

Viewgraph 8 shows two more simplified target vectors. The left plot represents steering to a single plane wave arriving from 10° below the horizontal. The right plot represents an alternating polarity array. This steering can be achieved by connecting sequences of array elements in alternating polarity. Such steering is of interest in matched field processing because the multiplication in the correlation process can be omitted and field vector points are only added or subtracted. This greatly reduces the computation load. The alternations of polarity here are chosen to

match those of the previous viewgraph.

The correlation function over the field will now be shown for these target vectors. Viewgraph 9 shows contours for matching to a 10° upcoming wave. The 0.4 contour here covers about the same area as the same contour did in the cz matched field shown earlier. The 0.2 contour here spreads out substantially farther than did the similar one of the cz case. Note that very little of the downgoing part of the cz correlates with this target vector.

Viewgraph 10 shows the 0.2 contour only for the target vector created by $\pm 10^\circ$ plane waves. This contour is much narrower than the previous for a single 10° plane wave, but the two sections of the cz are almost equally correlated.

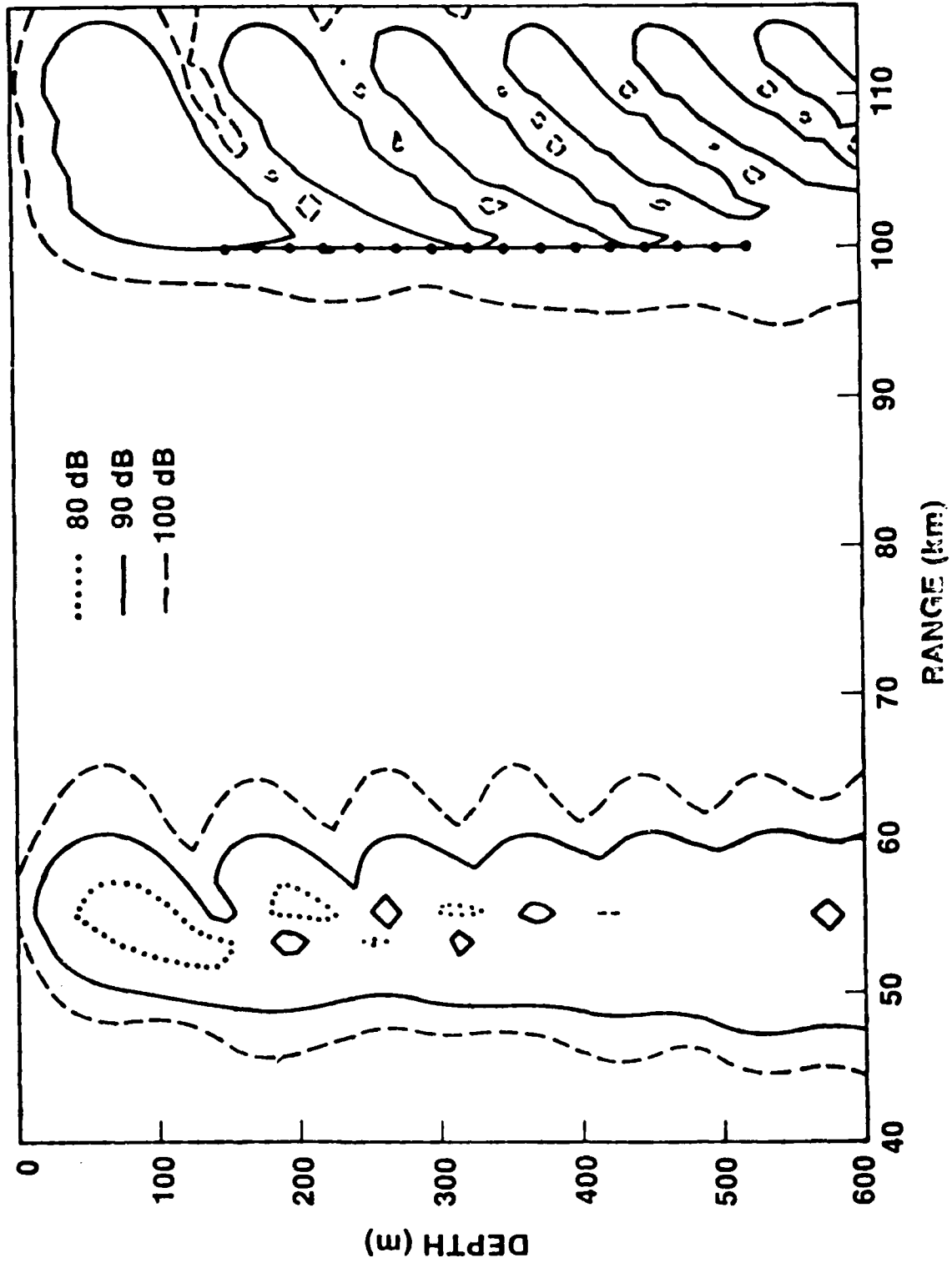
Finally, viewgraph 10 for the alternating polarity steering shows correlations that are similar but not as sharp as the previous case. An application of this concept would be observing only the relative phase down an array, quantizing to + and - and then adding or subtracting the computed field vectors to obtain the correlation.

In conclusion: Simulations show that if field matching at 30 Hz were attempted with a field computed only from cz energy, correlation functions would be broad and smooth, but would not peak at the true source depth. Further, secondary peaks would be found at locations in the cz where arrival patterns are in some way similar.

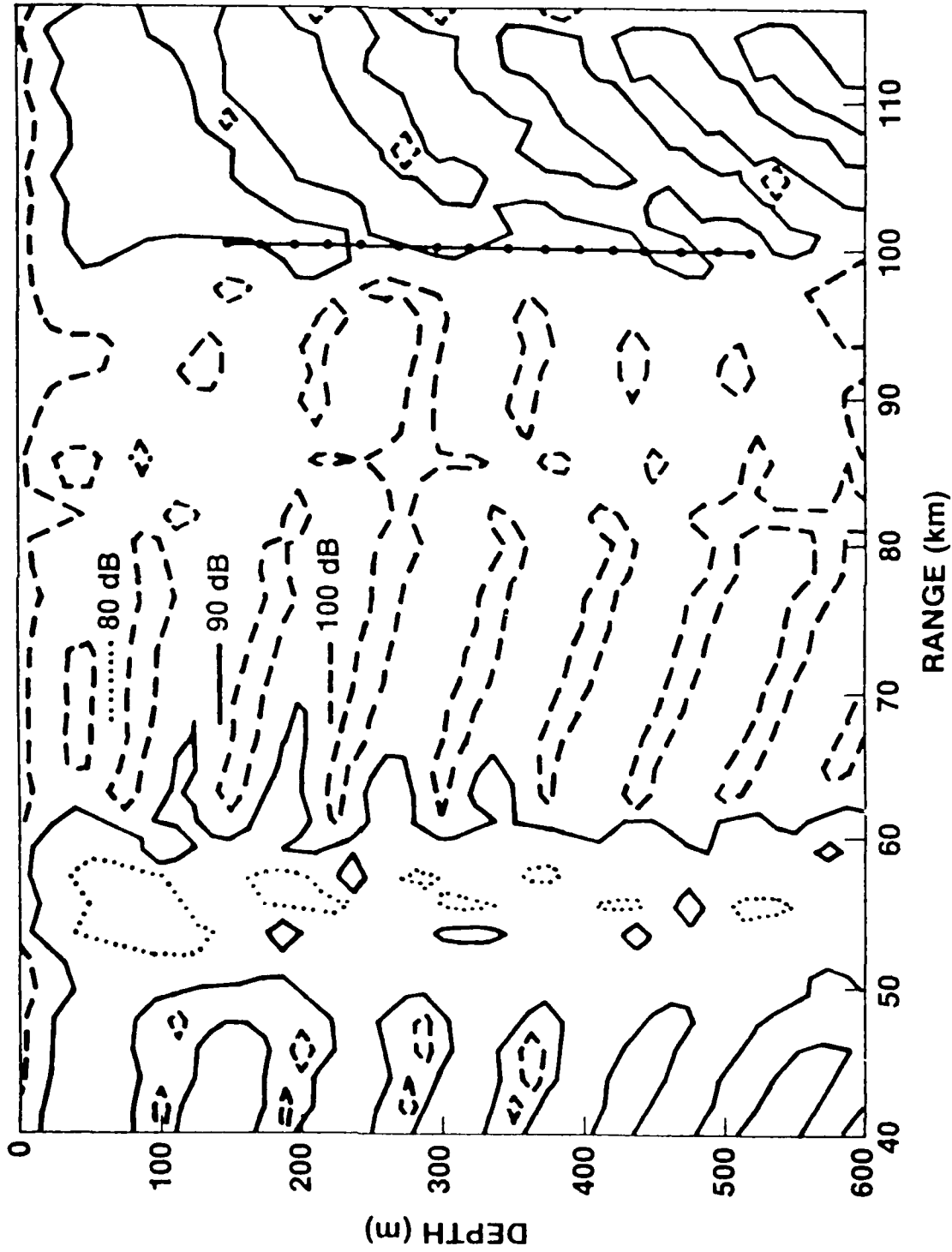
It is shown that results quite similar to those obtained by using the cz field could be obtained by methods similar to plane wave steering and even alternating polarity steering.



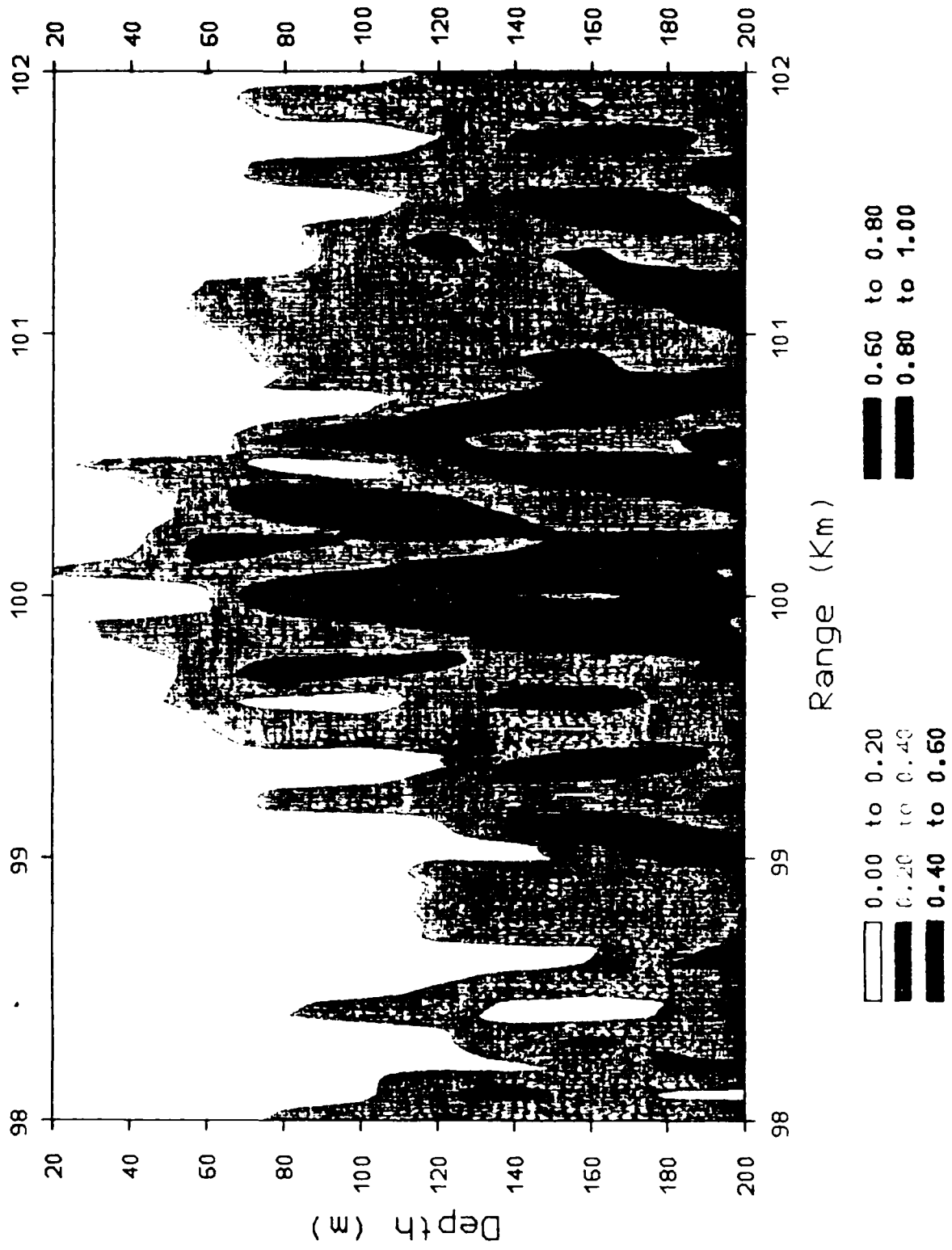
Propagation Loss Contours for Convergence Zone Modes Only



Propagation Loss Contours for Total Field

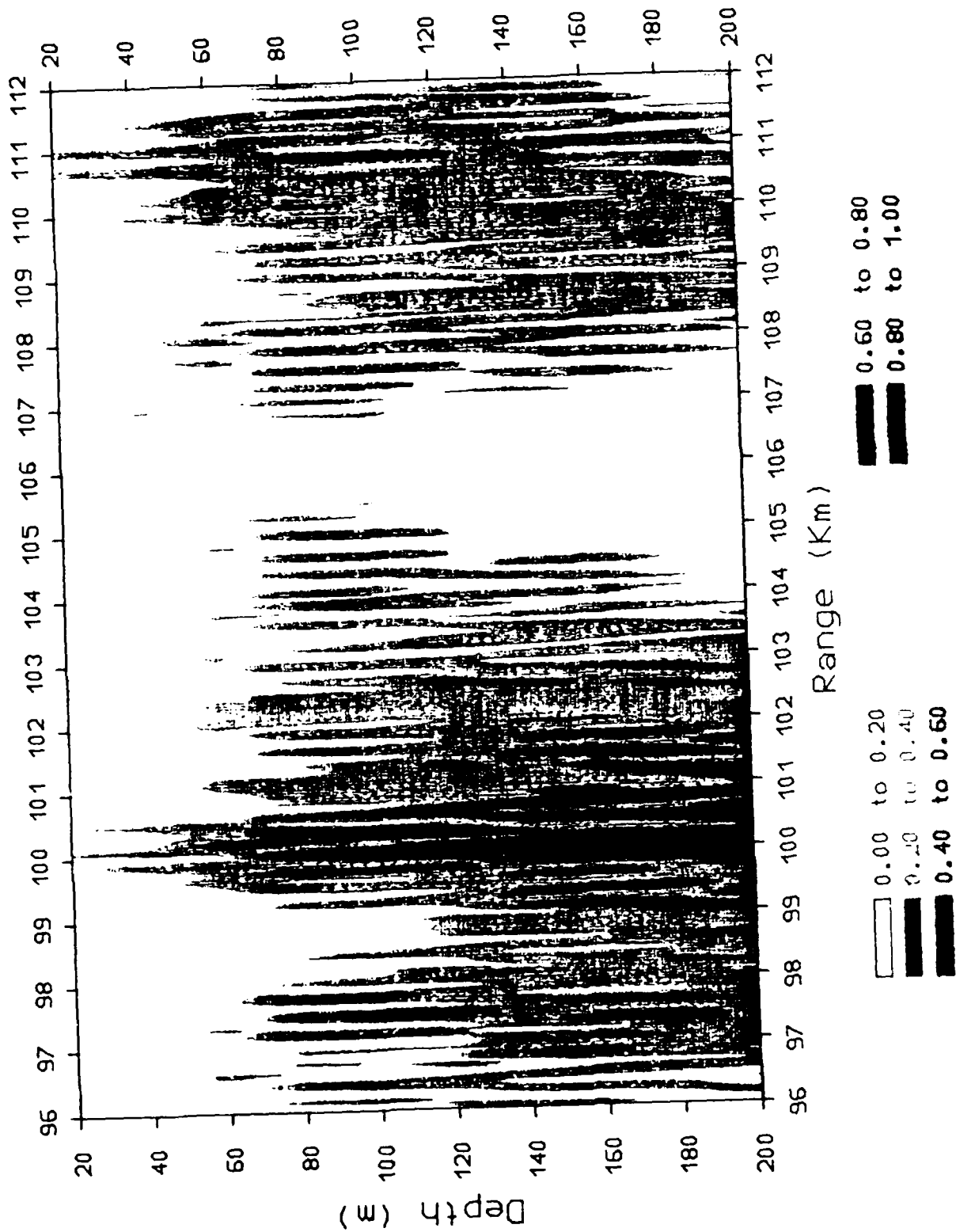


Matched-Field Correlation Coefficients for Total Field

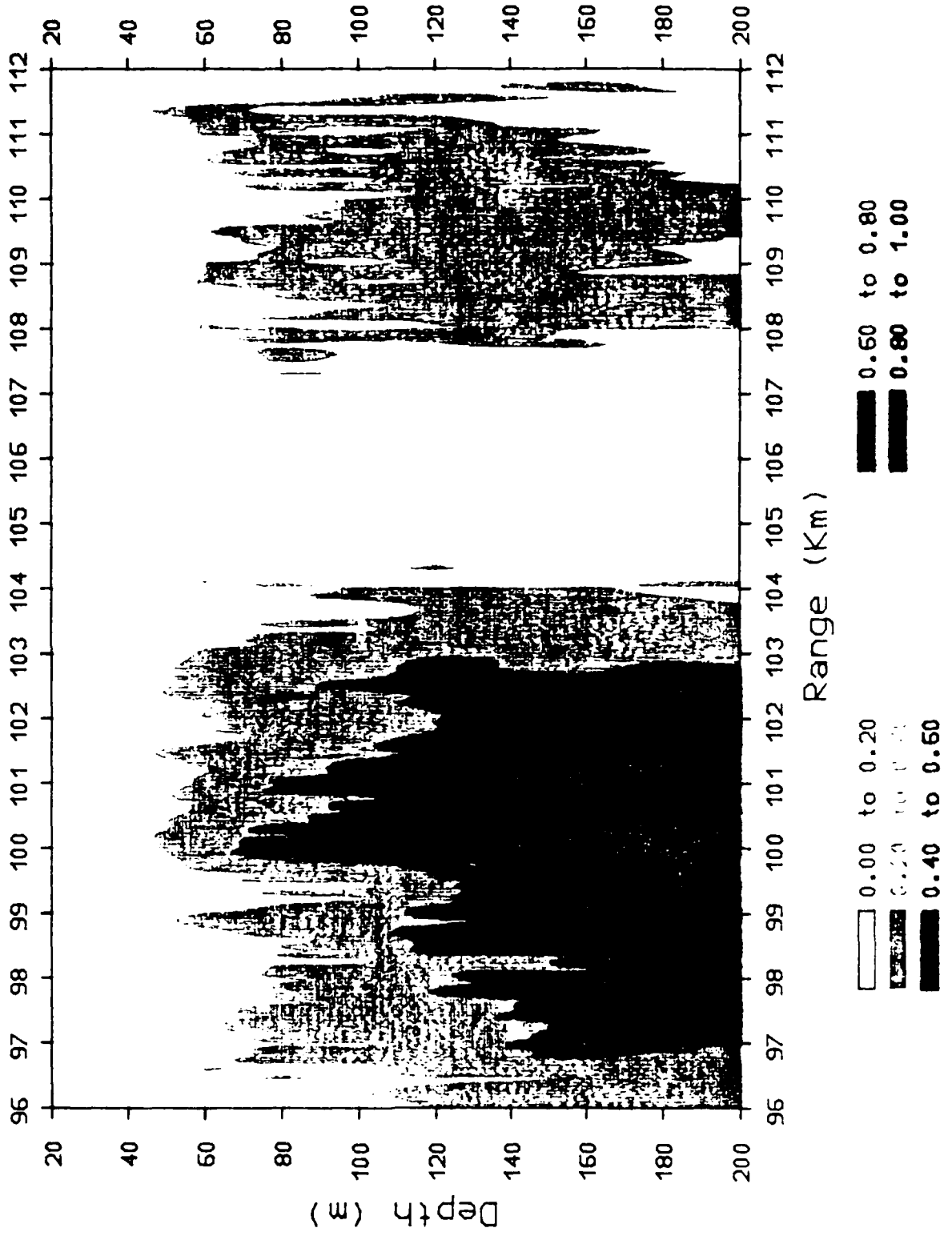




Matched-Field Correlation Coefficients for Total Field



Matched-Field Correlation Coefficients for Convergence Zone Target Vector



Two Ways to View the Correlation Process

Correlation

$$c(r, z) = \frac{\sum t_i p_i^*(r, z)}{[(\sum t_i t_i^*)(\sum p_i(r, z) p_i^*(r, z))]^{1/2}}$$

A. Matched Field

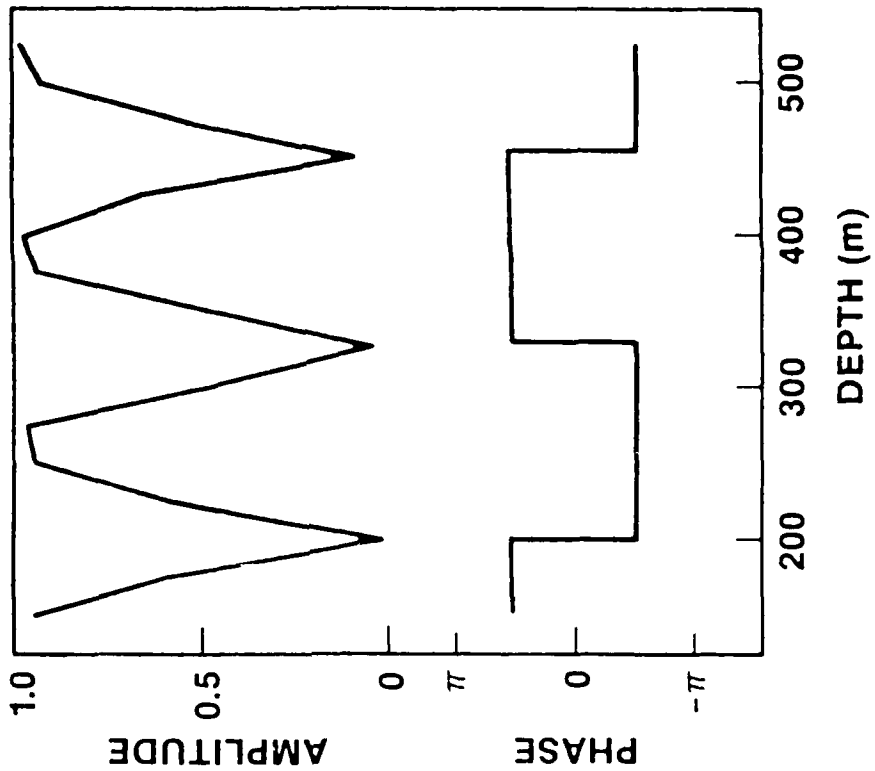
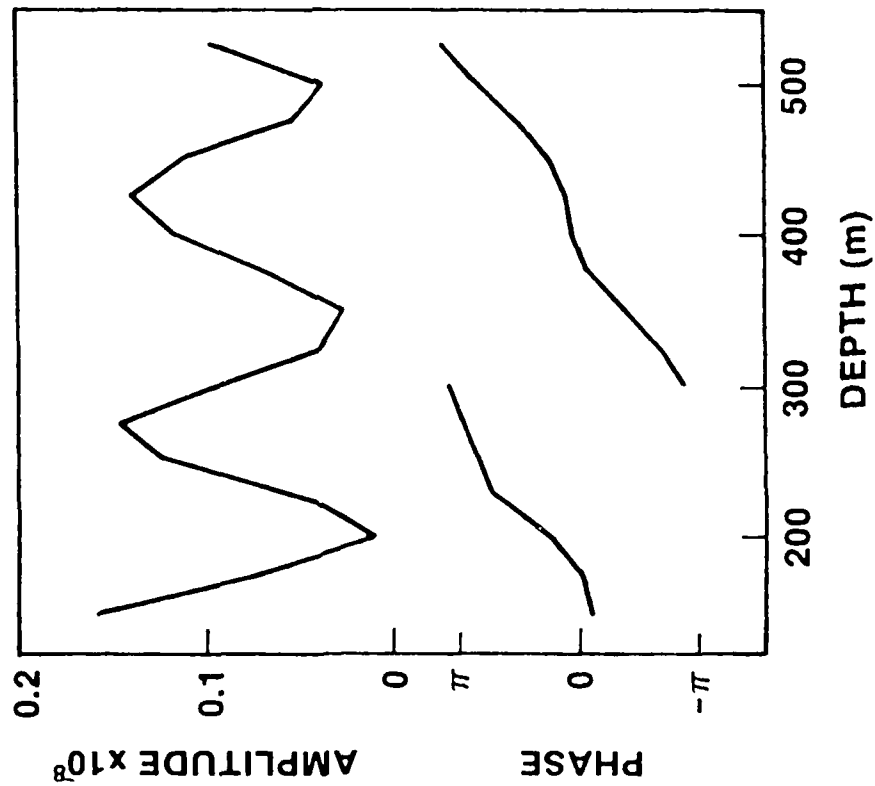
t = target vector

B. Beamforming

$$t_i = w_i \exp j \frac{[(i - 1) 2\pi d \sin \theta]}{\lambda}$$

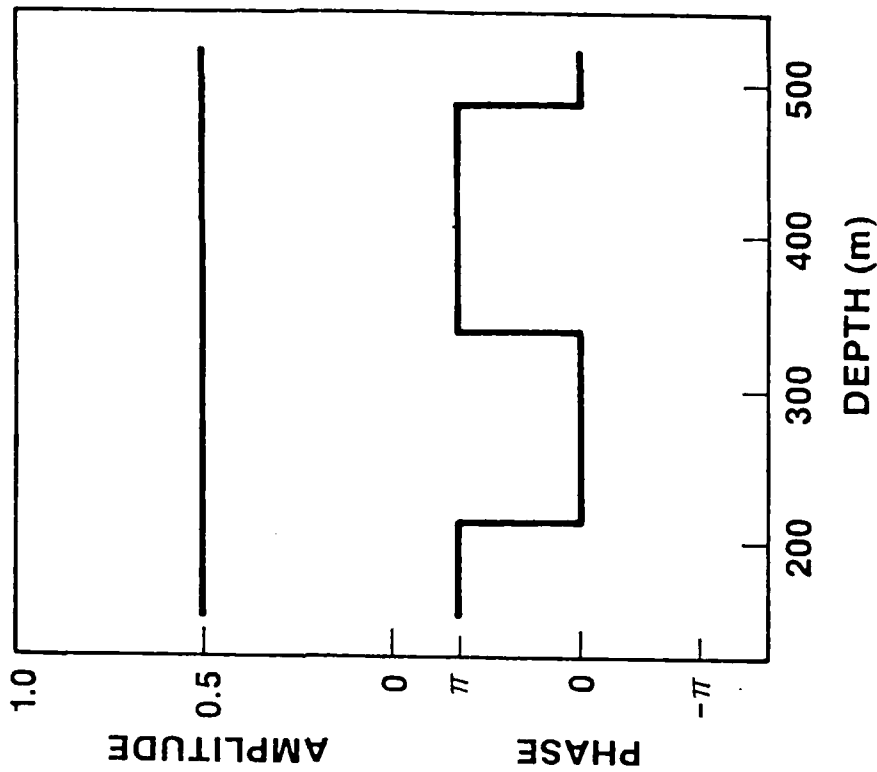
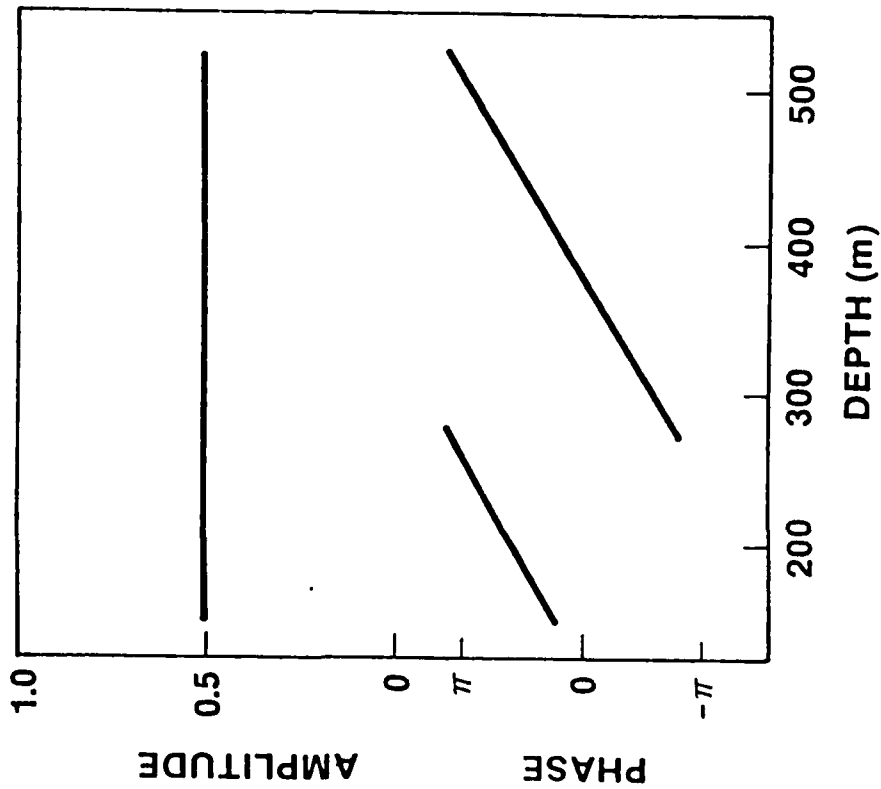
NOSCA

Sound Pressures at Array Depths for a Convergence Zone Computation and for Two Interfering Plane Waves



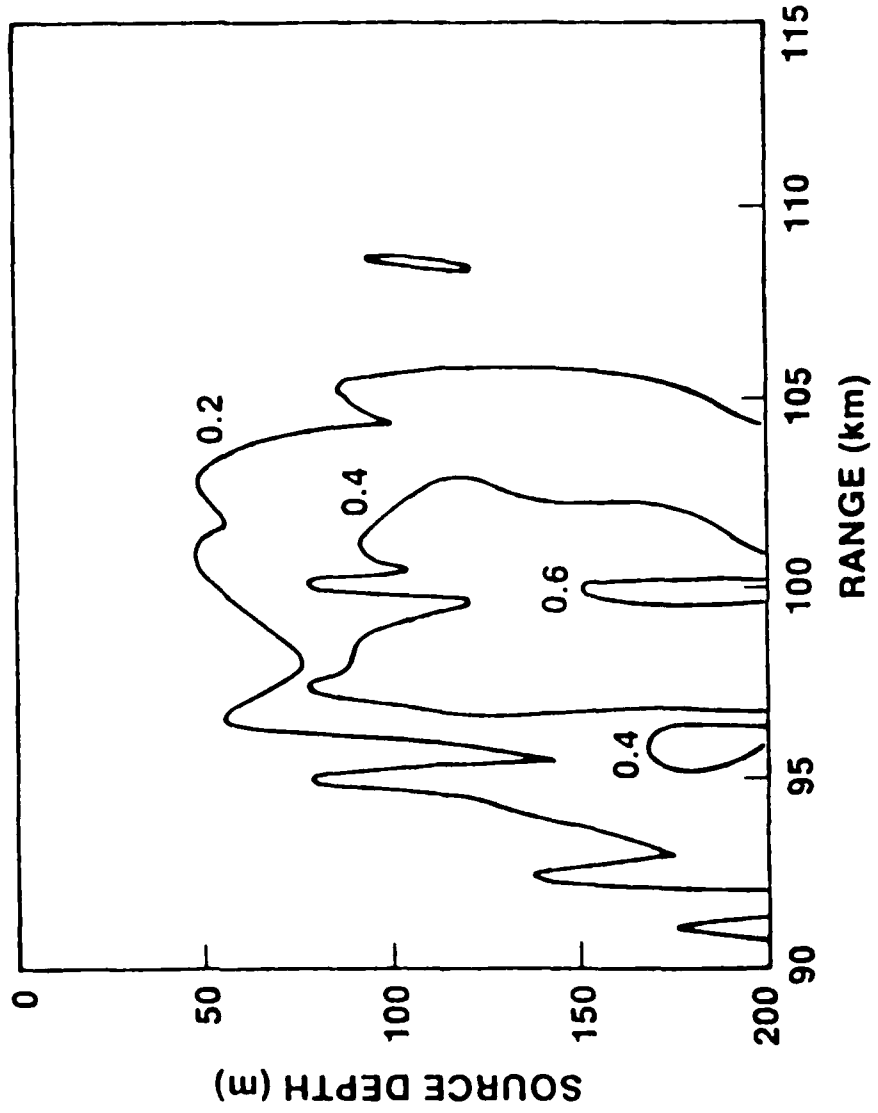


Sound Pressures at Array Element Depths for a 10° Upgoing Plane Wave and an Alternating Polarity Array



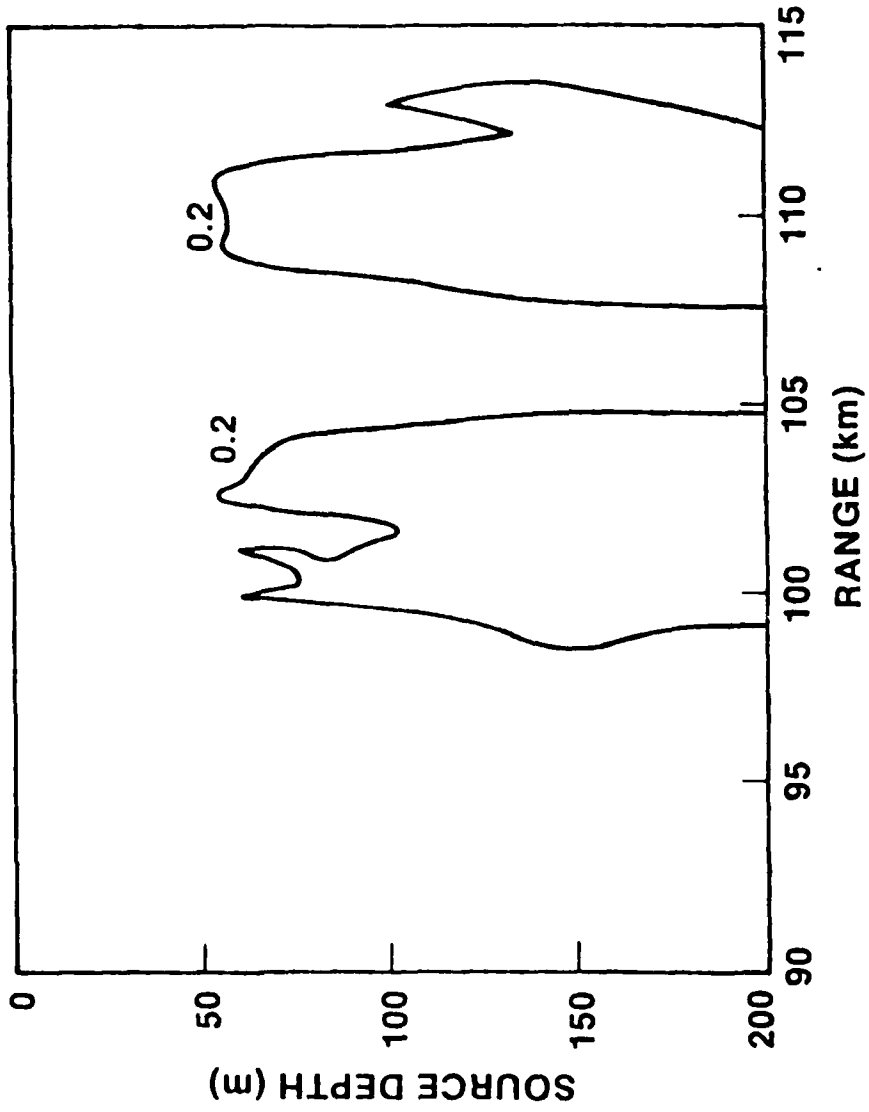
NOSCC

Correlation Contour for 10° Upgoing Plane Wave



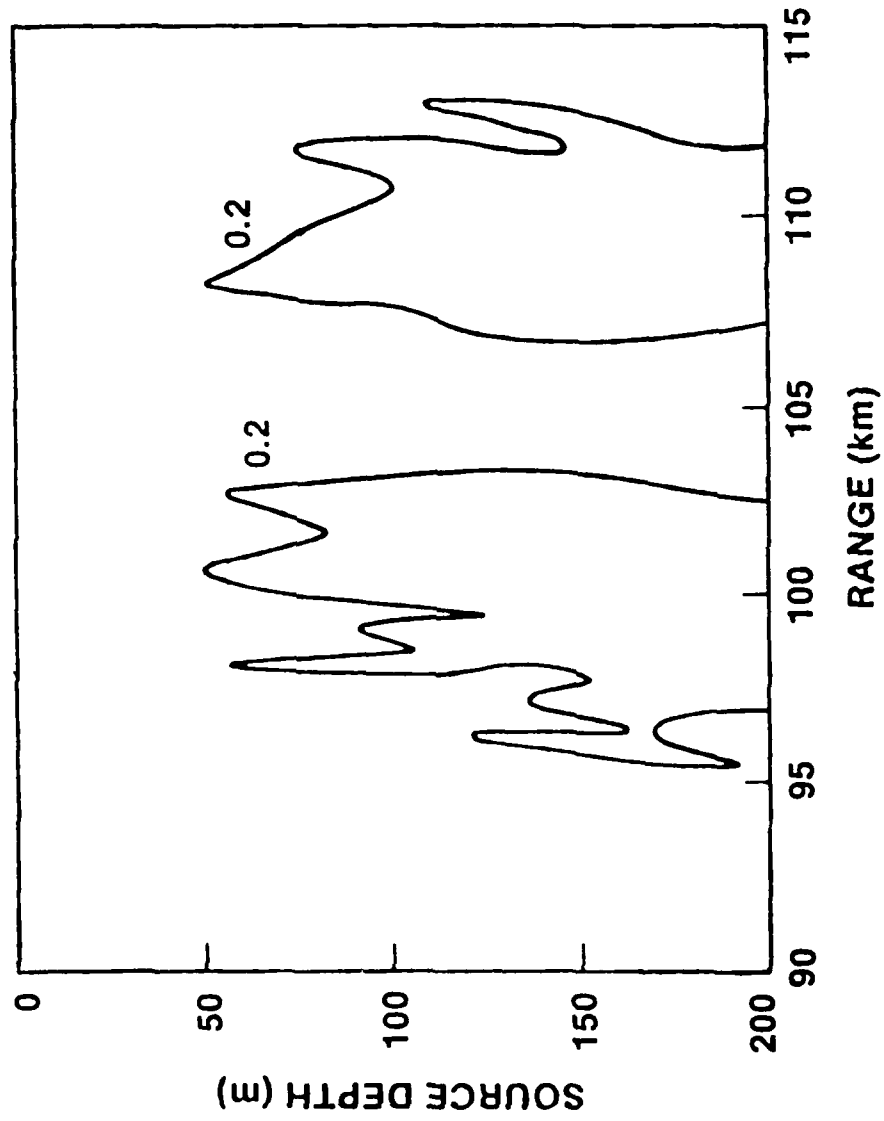


Correlation Contours for Up and Downgoing Plane Waves at 10°





Correlation Contours for Alternating Polarity Steering



END

DATE

FILMED

5-88

DTIC